High-frequency correction to the detector response and its effect on searches for gravitational waves

M Rakhmanov[1], J D Romano[1,2] and J T Whelan[3]

[1] University of Texas at Brownsville, Brownsville, Texas, 78520, USA
[2] Cardiff University, Cardiff CF24 3AA, Wales, UK
[3] Max-Planck-Institut für Gravitationsphysik (Albert-Einstein-Institut), Potsdam, GDR

E-mail: malik@phys.utb.edu, joe@phys.utb.edu, john.whelan@aei.mpg.de

Abstract. In a recent paper (CQG 21 (2004) 4041), Baskaran and Grishchuk noted that frequency corrections, resulting from the photon round trips between the test masses, contribute noticeably to the response of laser gravitational-wave detectors. They calculate these corrections for a simple Michelson interferometer and suggest that for ground-based detectors one can use a linear-frequency approximation to the exact response formula. They also point out that these corrections can be as large as 10 percent at a frequency of 1.2 kHz, and therefore can introduce significant systematic errors in current searches for gravitational waves with LIGO and VIRGO detectors. In this paper we re-examine these results. We show that even for ground-based detectors, accurate analysis requires the exact formula rather than the linear approximation. Using the exact formula, we re-evaluate the effect of the frequency-dependent terms and show that the corrections to the magnitude of the detector response are negligible (typically at a sub-percent level). However, the corrections to the phase can be significant (6 degrees at 1.2 kHz). We also extend the calculations to include the effect of Fabry-Perot resonators in the interferometer arms. In particular, we show that a simple approximation which combines the long-wavelength Michelson response with the single-pole approximation to the Fabry-Perot response produces rather accurate results. Finally, we estimate the errors that arise if one uses the long-wavelength approximation in searches for periodic gravitational-waves emitted e.g., by a known pulsar and in searches for an isotropic stochastic gravitational-wave background. For frequencies of order 1 kHz, the errors arising from the long-wavelength approximation are much less than one percent for searches performed so far. The correction to the planned LIGO Hanford-Livingston cross-correlation search for a stochastic background near 1 kHz is approximately 4 percent.

PACS numbers: 04.80.Nn, 95.55.Ym

1. Introduction

Searches for gravitational waves are currently conducted with km-scale laser interferometers such as LIGO [1] and VIRGO [2]. These detectors utilize a Michelson configuration which is further enhanced by the addition of Fabry-Perot cavities in the interferometer arms. Development of efficient data analysis algorithms requires accurate knowledge of the response of these detectors to gravitational waves. Historically, there were two widely used approaches to calculate the detector response. In one approach, it is assumed that the size of the detector is much less than

the wavelength of the incoming gravitational wave, and therefore can be neglected in the calculations. This approximation is often called the *long-wavelength* regime [3]. The advantage of this approach is that it allows one to interpret the effect of gravitational waves in terms of the motion of the test masses, appealing to our physical intuition. In another approach, one does not make any assumptions about the size of the detector compared to the wavelength of the incoming gravitational wave [4, 5]. Such calculations lead to a more accurate detector response, but are often considered unnecessary for ground-based detectors. It was pointed out by Baskaran and Grishchuk [6] that the long-wavelength approximation can lead to noticeable errors in the estimation of the parameters of the gravitational wave. In particular, they showed that the error in searches for periodic gravitational waves can be as large as 10% thus exceeding the uncertainties in the calibration proceedure, which currently are at the level of 5% [7]. This observation questioned the validity of the long-wavelength approximation and led to the necessity of estimating its impact on the search results. Two points of this analysis however required clarification. First, the authors assumed that for ground-based detectors it suffices to use the first-order correction to the long-wavelength approximation thus introducing a linear-frequency detector response, whereas the exact (non-linear) formula was readily available (and also derived in their paper). Second, they did not include the transfer function of Fabry-Perot cavities in the interferometer arms which play a crucial role in the formation of the signal for LIGO and VIRGO. We are now going to fill in these gaps.

In this paper we re-evaluate the errors due to the long-wavelength approximation and assess their impact on the current searches for gravitational waves with km-scale laser interferometers. We will show that the linear approximation breaks down for certain directions on the sky, and that even for ground-based detectors one should use the exact formula to capture the frequency-dependence of the response. We will also include the transfer function of the Fabry-Perot cavities in the interferometer arms and show that it leads to significant modification of the results. Finally, we estimate the errors from using the long-wavelength approximation in searches for periodic gravitational waves and in searches for an isotropic stochastic gravitational-wave background. We will show that in most cases the errors are negligible.

2. Michelson interferometer response (long-wavelength regime)

In the transverse-traceless gauge [3], a plane gravitational wave coming from direction $\hat{n}$ is given by

$$h_{ij}(t,\vec{x}) = h_+(t,\vec{x})\, e^+_{ij}(\hat{n}) + h_\times(t,\vec{x})\, e^\times_{ij}(\hat{n})\,, \tag{1}$$

where $h_{+,\times}(t,\vec{x}) = h_{+,\times}(t+\vec{x}\cdot\hat{n}/c)$, and the polarisation tensors are defined by

$$e^+_{ij}(\hat{n}) = \ell_i\ell_j - m_i m_j, \tag{2}$$

$$e^\times_{ij}(\hat{n}) = \ell_i m_j + m_i \ell_j\,. \tag{3}$$

Here $\hat{\ell}$, $\hat{m}$ are chosen so that $(\hat{\ell},\hat{m},\hat{n})$ is a right-handed orthonormal basis. (There is rotational freedom associated with the choice of $\hat{\ell}$, $\hat{m}$.)

Consider a simple Michelson interferometer with arms aligned along the unit vectors $\hat{a}$ and $\hat{b}$. In the long-wavelength limit ($L/\lambda \to 0$), a gravitational wave produces a signal in the interferometer [8, 9]:

$$V(t) = \frac{1}{2}(a^i a^j - b^i b^j) h_{ij}(t,\vec{0})\,, \tag{4}$$

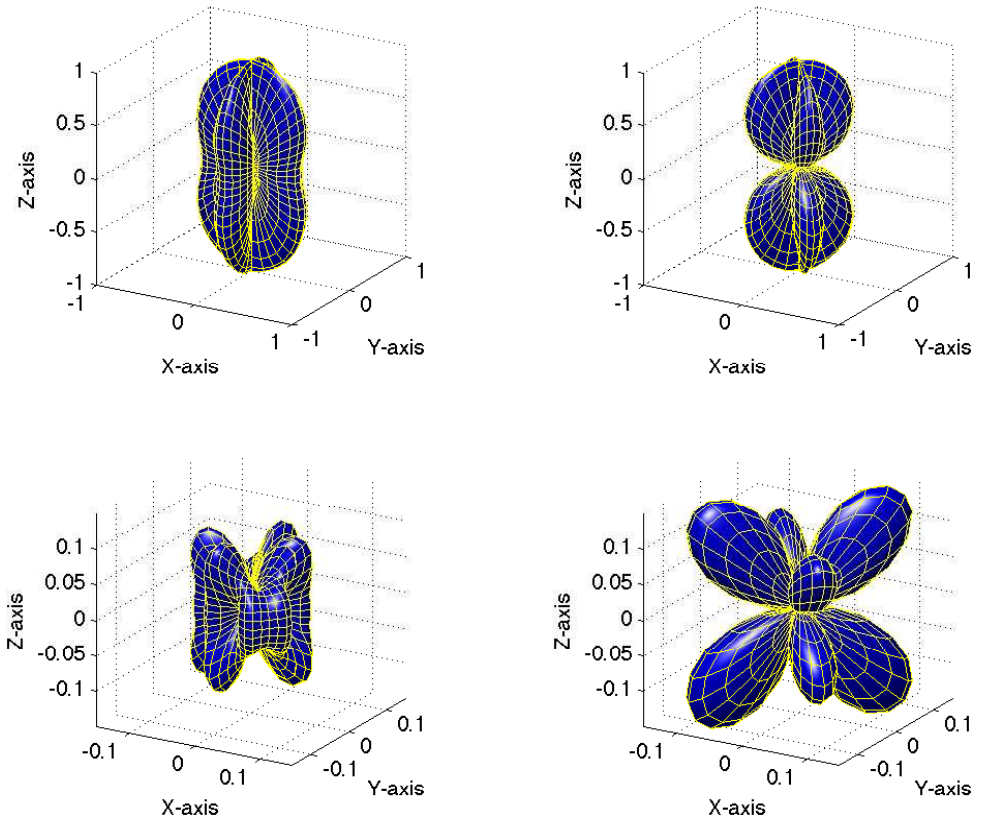

Figure 1. Top: antenna patterns in the long-wavelength approximation, $|F_+(\hat{n})|$ [left panel] and $|F_\times(\hat{n})|$ [right panel]. Bottom: antenna patterns at the FSR ($f = 37.5$ kHz), $|G_+(\hat{n}, f)|$ [left panel] and $|G_\times(\hat{n}, f)|$ [right panel] (see Sec. 3.2).

or equivalently,

$$V(t) = F_+(\hat{n})h_+(t) + F_\times(\hat{n})h_\times(t)\,, \tag{5}$$

where

$$F_A(\hat{n}) = \frac{1}{2}\,(a_i a_j - b_i b_j)e^{ij}_A(\hat{n}) \tag{6}$$

are the interferometer responses to the two independent polarisations ($A = +, \times$) of the gravitational wave. In the frequency domain, (5) becomes

$$\tilde{V}(f) = F_+(\hat{n})\tilde{h}_+(f) + F_\times(\hat{n})\tilde{h}_\times(f)\,, \tag{7}$$

where tilde denotes Fourier transform with respect to t.

Three-dimensional representations of the absolute value of F_A as a function of $\hat{n}$ are often called *antenna patterns*. Antenna patterns have traditionally been plotted for a particular choice of polarisation basis. Figure 1 (top panels) show the long-wavelength antenna patterns $F_{+,\times}(\hat{n})$ for $\hat{a} = \hat{x}$, $\hat{b} = \hat{y}$ and a polarisation basis defined by $\hat{\ell} = -\hat{\phi}$, $\hat{m} = \hat{\theta}$, where $\hat{\theta}$, $\hat{\phi}$ are the standard unit vectors tangent to a unit sphere.

3. Michelson interferometer response (exact formula)

Taking into account the finite size of the detectors leads to *frequency-dependent* detector responses as shown for example in early calculations for LIGO [4, 10, 11, 12, 13, 14] and LISA [15, 16, 17]. The detector output is now a convolution in the time domain, which is more conveniently expressed in the frequency domain as

$$\tilde{V}(f) = H_+(\hat{n}, f)\tilde{h}_+(f) + H_\times(\hat{n}, f)\tilde{h}_\times(f)\,. \tag{8}$$

Here we briefly derive the detector responses $H_A(\hat{n}, f)$ following [13, 14].

3.1. Photon round-trip time

The interval for a photon propagating in the gravitational-wave background is

$$ds^2 = -c^2dt^2 + [\delta_{ij} + h_{ij}(t, \vec{x})]\, dx^i dx^j = 0\,. \tag{9}$$

Consider a round-trip for photons launched along a single arm $\hat{a}$ of a gravitational-wave detector. The unperturbed trajectory for photons is $x^i = a^i\xi$, where ξ is the parameter along the trajectory: $\xi = 0$ to L for forward propagation, and $\xi = L$ to 0 for the return trip. Substituting this trajectory in (9) and solving for t, we obtain

$$c(t - t_0) = \int_0^\xi \left(1 + h_{ij}\, a^i a^j\right)^{1/2} \mathrm{d}\xi'. \tag{10}$$

Let T be the nominal (unperturbed) photon transit time: $T \equiv L/c$. In the presence of a gravitational wave, the transit time will slightly deviate from its nominal value giving: $T_{1,2} = T + \delta T_{1,2}$. For forward propagation

$$\delta T_1(t) = \frac{1}{2c} a^i a^j \int_0^L h_{ij}\left(t_0 + \frac{\xi}{c} + \frac{\hat{n}\cdot\hat{a}}{c}\xi\right) \mathrm{d}\xi, \tag{11}$$

where t_0 is the starting time for the photon propagation which can be approximated by $t_0 = t - T$. For the return trip,

$$\delta T_2(t) = \frac{1}{2c} a^i a^j \int_0^L h_{ij}\left(t_0 + \frac{L - \xi}{c} + \frac{\hat{n}\cdot\hat{a}}{c}\xi\right) \mathrm{d}\xi. \tag{12}$$

Here too t_0 can be approximated by $t_0 = t - T$. The total change of the photon propagation time during one round trip, $\delta T_{\mathrm{r.t.}}(t)$, can be found by adding $\delta T_2(t)$ with $\delta T_1[t - T_2(t)]$, where $T_2(t)$ can be replaced with T to first order in h. Taking the Fourier transform of $\delta T_{\mathrm{r.t.}}(t)$, we obtain

$$\frac{\delta\tilde{T}_{\mathrm{r.t.}}(f)}{T} = D(\hat{a}, f)\, a_i a_j e_A^{ij}(\hat{n})\tilde{h}_A(f)\,, \tag{13}$$

where we introduced the transfer function

$$D(\hat{a}, f) = \frac{e^{-i2\pi fT}}{2}\left[e^{i\pi fT_+}\mathrm{sinc}\,(\pi fT_-) + e^{-i\pi fT_-}\mathrm{sinc}\,(\pi fT_+)\right]\,, \tag{14}$$

with short-hand notation $T_\pm \equiv T(1 \pm \hat{a}\cdot\hat{n})$.

3.2. Phase shift of a continuous wave

For continuous laser light with intrinsic angular frequency ω_0, the delay due to gravitational waves leads to a phase shift $\psi = \omega_0 \delta T$. Superposition of the two beams in a Michelson interferometer will produce a signal in the dark port proportional to the differential phase $V(t) \equiv \psi(t)/\omega_0 T$. In the frequency domain, the signal has the general form (8) with $H_A(\hat{n}, f)$ given by

$$G_A(\hat{n}, f) = \frac{1}{2}\left[D(\hat{a}, f)\, a_i a_j - D(\hat{b}, f)\, b_i b_j\right] e_A^{ij}(\hat{n})\,. \tag{15}$$

These are simply differences of the single-arm detector responses (13) for the two arms $\hat{a}$ and $\hat{b}$. Figure 1 (bottom) is a plot of the magnitude of the detector response functions $G_A(\hat{n}, f)$ at the FSR ($f = 37.5$ kHz). Note the presence of additional lobes and a factor of 5-8 reduction in overall amplitude relative to the long-wavelength antenna patterns in figure 1 (top two panels). The long-wavelength approximation (6) is a special case of these response functions:

$$F_A(\hat{n}) = G_A(\hat{n}, f)|_{f=0}\,, \tag{16}$$

indicating that a more appropriate naming convention would be *infinite-wavelength* approximation.

3.3. Magnitude of frequency corrections

In [6], Baskaran and Grishchuk considered a first-order approximation to the exact response function:

$$G_A(\hat{n}, f) \approx G_A(\hat{n}, 0) + f\,\frac{\partial G_A}{\partial f}(\hat{n}, 0)\,, \tag{17}$$

and suggested that is sufficient for ground-based gravitational-wave detectors. They estimate the magnitude of this linear correction for a periodic gravitational-wave signal, and find that it is approximately 10% for a frequency of 1.2 kHz. For comparison, the uncertainties in the current calibration proceedure are approximately 5% [7]. Therefore, it is worthwhile to review these results.

We notice that the Taylor expansion in (17) is problematic because its coefficients are functions of the source location—i.e., depend on $\hat{n}$. One can see that the derivative vanishes for some locations in the sky. Similar calculation of the second-order term, proportional to the second derivative, shows that it remains finite at these locations. At these places, the approximation (17) breaks down no matter how small the frequency is. We therefore conclude that even for ground-based detectors one should use the exact formula (15), rather than the linear approximation (17), to capture the frequency-dependence of the response.

The magnitude of the error from using the long-wavelength approximation in place of the exact formula is given by

$$|G_A(\hat{n}, f) - F_A(\hat{n})|. \tag{18}$$

This quantity is shown in figure 2 (middle two panels) for $f = 1024$ Hz. Indeed, the largest value for this error is approximately 0.1, which constitutes a 10% effect when compared with the maximum value of $|F_A|$. (The top two panels are simply a different representation of long-wavelength antenna patterns in figure 1 (top).) To understand the meaning of this error, we also consider another quantity,

$$|G_A(\hat{n}, f)| - |F_A(\hat{n})|, \tag{19}$$

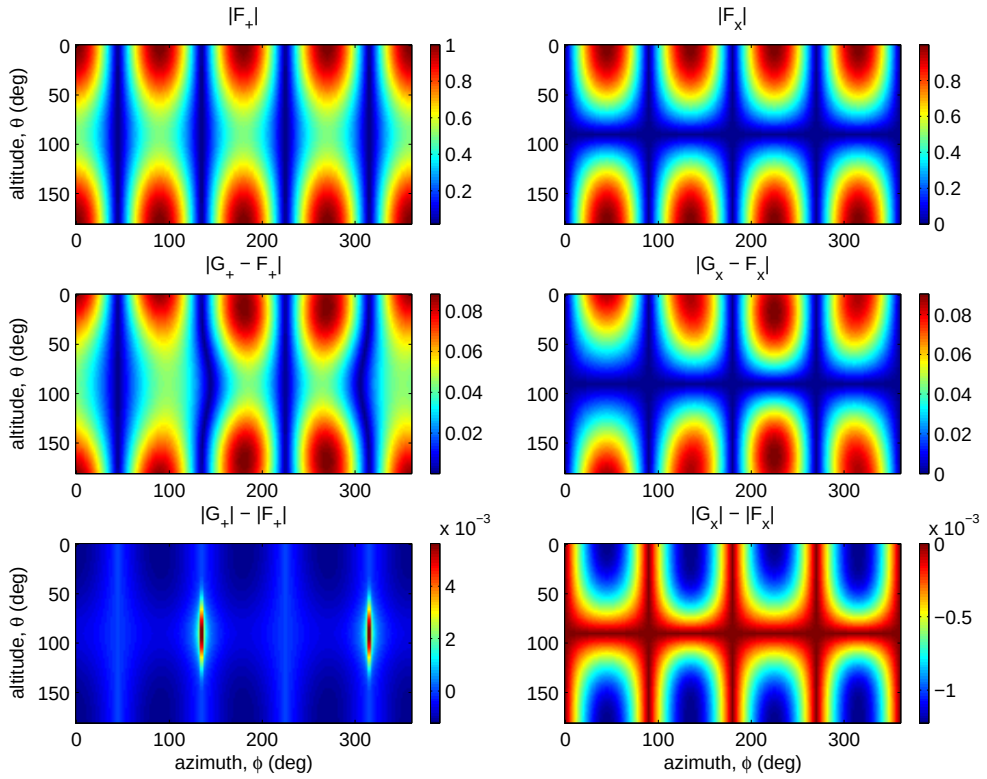

Figure 2. Top: magnitude of the long-wavelength detector response functions $|F_A|$, middle: magnitude of the difference $|G_A - F_A|$, bottom: difference of the magnitudes $|G_A| - |F_A|$, all at $f = 1024$ Hz.

which is shown figure 2 (bottom). Note that the largest absolute value for this quantity is less than 1%. This implies that the magnitude of the detector response is not affected by the frequency corrections. Therefore, the effect of such corrections is almost entirely in the phase of the response. The majority of this can be explained by the delay due to the photon transit in the arms, a factor of $e^{-i2\pi fT}$ in (14). Note that this factor is not included in [6].

4. Effect of Fabry-Perot arm cavities

The presence of Fabry-Perot cavities in the interferometer arms adds further filtering of the signal. If the amplitude of the light incident on the cavity is A_0 and the phase of the light in one round-trip is $\psi(t)$, the multi-beam interference leads to

$$E(t) = t_1 A_0 \sum_{k=0}^{\infty} (r_1 r_2)^k e^{i\psi(t-2kT)}\,, \tag{20}$$

where $r_{1,2}$ and t_1 are the reflectivity and transmissivity of the cavity mirrors. Let the amplitude and the phase of this field be A and Ψ: $E = Ae^{i\Psi}$. Approximating $e^{i\psi} \approx 1 + i\psi$ in (20), and keeping only first order terms, we obtain that the amplitude

of the field in the cavity is $A = t_1 A_0/(1 - r_1 r_2)$ and its phase is given by

$$\Psi(t) = (1 - r_1 r_2) \sum_{k=0}^{\infty} (r_1 r_2)^k \psi(t - 2kT) \,. \tag{21}$$

Equivalently, in the Fourier domain

$$\tilde{\Psi}(f) = C(f)\tilde{\psi}(f) \,, \qquad C(f) = \frac{1 - r_1 r_2}{1 - r_1 r_2 e^{-i4\pi fT}} \,. \tag{22}$$

Thus, the filtering properties of a Fabry-Perot cavity can simply be taken into account by multiplying the Michelson response (15) by the *direction-independent* transfer function $C(f)$. Defining $\tilde{V}(f) \equiv \tilde{\Psi}(f)/\omega_0 T$, we have

$$H_A(\hat{n}, f) = G_A(\hat{n}, f)\, C(f). \tag{23}$$

Note that the transfer function of the Fabry-Perot cavity can be also be written as

$$C(f) = e^{i2\pi fT} \frac{\sinh(2\pi f_0 T)}{\sinh[2\pi f_0 T(1 + if/f_0)]} \,, \tag{24}$$

where f_0 is the lowest order pole, $f_0 \equiv -\ln(r_1 r_2)/(4\pi T)$. For the 4-km LIGO detectors, $f_0 \approx 86$ Hz.

At $f = 0$, the response of a Michelson-Fabry-Perot interferometer (23) reduces to the standard long-wavelength responses (6). For finite, but low frequencies ($2\pi fT \ll 1$), one can improve upon this approximation by simply multiplying the long-wavelength formulae (6) by a phase factor $e^{-i2\pi fT}$ to take into account the delay due to the photon transit time in the interferometer arm, and using the lowest-order single-pole approximation for the Fabry-Perot response function:

$$C(f) \approx e^{i2\pi fT} C_{\rm pole}(f) \,, \qquad C_{\rm pole}(f) = \frac{1}{1 + if/f_0} \,. \tag{25}$$

Thus,

$$H_A(\hat{n}, f) \approx C_{\rm pole}(f)\, F_A(\hat{n}) \,. \tag{26}$$

Note that simply approximating the exact Fabry-Perot response function $C(f)$ with the single-pole transfer function $C_{\rm pole}(f)$ leads to errors in phase as large as 10 degrees at $f = 2$ kHz; approximating $C(f)$ as in (25) leads to much smaller errors.

5. Effect on searches for periodic gravitational waves

A gravitational-wave signal from a pulsar is largely periodic (with center frequency f) and therefore would greatly benefit from synchronous detection (heterodyne method) [18]. Taking into account the frequency-dependence of the detector response, the output of the heterodyne method is given by the following (complex) quantity

$$y(t) = \frac{1}{2} \left[H_+(\hat{n}, f; t) \frac{1}{2}(1 + \cos^2 \iota) - i H_\times(\hat{n}, f; t) \cos \iota \right] h_0 e^{i\phi_0} \,, \tag{27}$$

where h_0 is the amplitude, ι the inclination angle, and ϕ_0 the initial phase of the heterodyne method. The synchronous detection removes the dominant oscillatory part of the signal at the center frequency f, and also corrects for any phase modulation (Doppler shift) due to the rotation of the Earth and its orbital motion relative to the pulsar. The remaining time-dependence in y comes from the Earth's sidereal rotational motion. (The unit vectors $\hat{a}$, $\hat{b}$, which point along the detector arms, rotate with the Earth and are thus time-dependent in equatorial coordinates.)

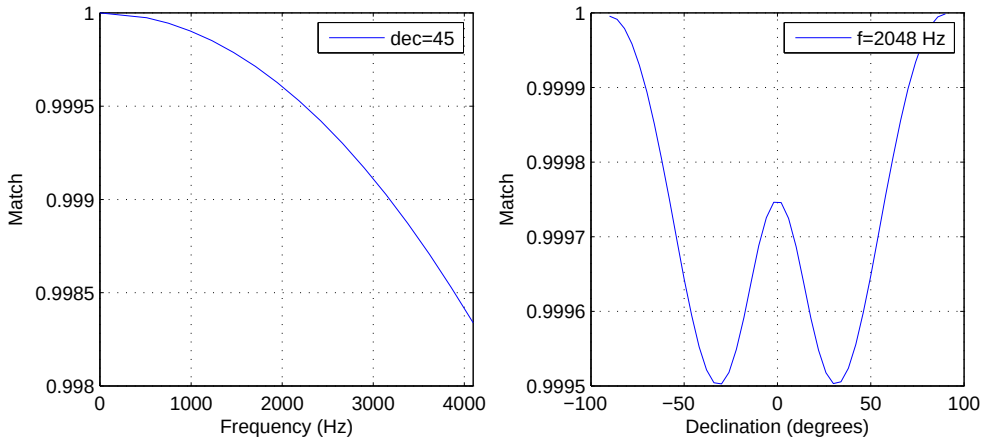

Figure 3. Fraction of maximum available signal-to-noise ratio (i.e., match) as a function of gravitational-wave frequency for fixed source declination (dec = 45°) [left panel], and as a function of source declination for fixed gravitational-wave frequency ($f = 2048$ Hz) [right panel].

The error associated with the use of the long-wavelength approximation for a Michelson-Fabry-Perot interferometer such as LIGO is given by

$$\text{match} = \frac{\frac{1}{2}\int (y_1 y_2^* + y_1^* y_2)\mathrm{d}t}{\sqrt{\int |y_1|^2 \mathrm{d}t}\,\sqrt{\int |y_2|^2 \mathrm{d}t}}\,, \tag{28}$$

where y_1 is the heterodyned signal (27) calculated using the exact response (23), and y_2 is the corresponding signal calculated using long-wavelength approximation (26). The match represents the fraction of maximum available signal-to-noise ratio. The integration time is one sidereal day. Figure 3 shows the match as a fuction of frequency f for fixed source declination (dec = 45°) [left panel], and the match as a function of declination for fixed frequency ($f = 2048$ Hz) [right panel] for the simple case where ψ, ι, and ϕ_0 are assumed to be known with values $\psi = 0$, $\iota = 0$, and $\phi_0 = 0$. This choice of parameters corresponds to a circularly-polarised gravitational wave. (The detector arms $\hat{a}$, $\hat{b}$ were taken to be those of H1 interferometer.) One can see that the reduction in signal-to-noise ratio is much less than 1% for all directions on the sky and for gravitational-wave frequencies up to 4 kHz. (A similar calculation, using the long-wavelength (6) and exact (15) expressions for a simple Michelson interferometer, leads to a reduction in signal-to-noise ratio of about 2% at 2 kHz, due primarily to the phase factor $e^{-i2\pi fT}$ in (14).) This rather simple example is representative of the size of the systematic errors introduced by the long-wavelength approximation on searches for periodic gravitational waves from known pulsars.

6. Effect on searches for stochastic gravitational waves

Assuming that the stochastic background is described by an isotropic, unpolarised, and Gaussian-stationary random process one can show [11, 19, 20] that the expected value of the cross-correlation for a superposition of random signals coming from all

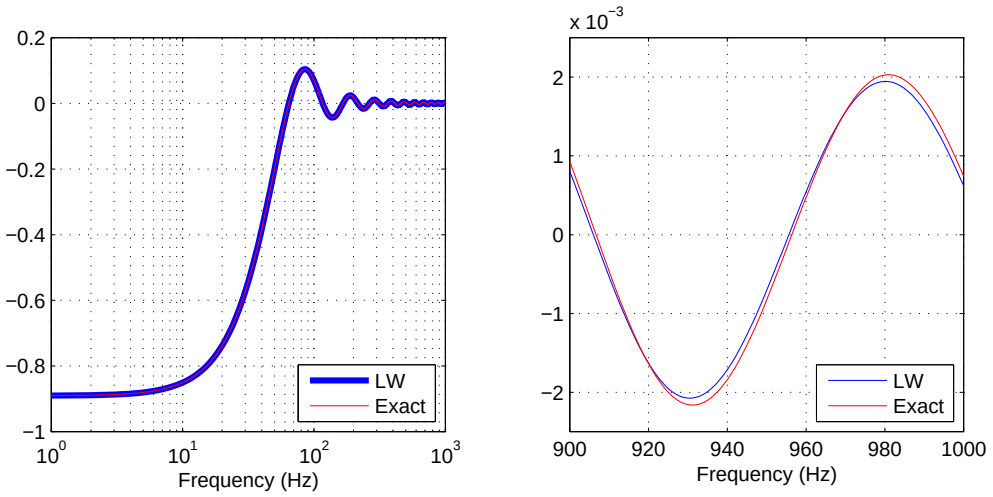

Figure 4. Overlap reduction function $\Gamma(f)$ for the two 4-km-long LIGO interferometers H1 and L1, calculated using the long-wavelength and exact detector response functions for a simple Michelson.

directions on the sky is proportional to the *overlap reduction function*:

$$\gamma(f) = \frac{5}{8\pi} \int_{S^2} \mathrm{d}^2\Omega_{\hat{n}} H^*_{1A}(\hat{n}, f) H_{2A}(\hat{n}, f) e^{-i2\pi f \hat{n}\cdot(\vec{x}_1 - \vec{x}_2)/c} \,, \tag{29}$$

where summation over polarisation indices A is understood. The overlap reduction function depends on the separation and relative misalignment of a pair of detectors located at $\vec{x}_1$ and $\vec{x}_2$, as well as on the individual detector response functions. Since it is often convenient to factor-out any *direction-independent* response functions from the integral in (29), we also define

$$\Gamma(f) = \frac{5}{8\pi} \int_{S^2} \mathrm{d}^2\Omega_{\hat{n}} G^*_{1A}(\hat{n}, f) G_{2A}(\hat{n}, f) e^{-i2\pi f \hat{n}\cdot(\vec{x}_1 - \vec{x}_2)/c} \,, \tag{30}$$

which depends only on the geometry of the detectors. A typical overlap reduction function $\Gamma(f)$ is shown in figure 4 for the two LIGO 4-km inteferometers (H1 and L1), calculated using both the long-wavelength (6) and exact expression (15) for the detector response functions for a simple Michelson. (An analogous plot for $\gamma(f)$ would have it wiggles suppressed at higher frequencies, due to the frequency dependence of the Fabry-Perot response functions (22) and (25).)

Using the explicit forms of the exact and long-wavelength detector response functions given in the previous sections, it is possible to derive analytic expressions for the overlap reduction function not only in the long-wavelength approximation [19], but also for the 1st-order corrections [14]. The one stochastic search so far influenced by kHz frequencies was the L1-ALLEGRO search, which involved cross-correlating the Livingston interferometer with the ALLEGRO bar detector in three different orientations [21]. Table 1 contains the relevant corrections to $\Gamma(f)$ at $f \approx 915\,\mathrm{Hz}$ due to the finite length of the L1 arms, using the long-wavelength (6) and exact expression (15) for the detector response functions for a simple Michelson. The upper limits in [21] were not affected to the stated precision by these corrections.

Table 1. Impact of corrections to the long-wavelength approximation on the LLO-ALLEGRO search. The corrections are less than 1%, except for the null orientation. The upper limits in [21] were not affected to the stated precision by these corrections.

	$\Gamma^{\rm LW}(f)$	$\delta\Gamma(f)$	$\delta\Gamma(f)/\Gamma^{\rm LW}(f)$
XARM	0.95333	−0.00089	−0.00093
YARM	−0.89466	0.00196	−0.00219
NULL	0.03181	−0.00073	−0.02305

Table 2. Corrections to the statistical error bars for pairs of interferometers resulting from use of the long-wavelength approximation. The numbers in the table are $\delta\sigma/\sigma$, calculated assuming a white stochastic backgrounds across the band shown, using the nominal design sensitivities of the instruments. The 4% correction for H1-L1 at 1 kHz is comparable to the current calibration uncertainties for these searches.

$f_{\rm min} - f_{\rm max}$	H1-L1	H1-V1	L1-V1
$50 - 150\,{\rm Hz}$	-1.9×10^{-3}	2.2×10^{-4}	2.8×10^{-4}
$900 - 1000\,{\rm Hz}$	-4.1×10^{-2}	2.8×10^{-3}	2.8×10^{-3}

Previous H1-L1 and H2-L1 correlation analyses have concentrated on frequencies $f \lesssim 300\,{\rm Hz}$, but inclusion of the 3-km long VIRGO interferometer (V1) in LIGO's 5th science run (S5) has added interest in frequencies around 1 kHz. A typical measure of the impact of corrections to the low-frequency approximation is the fractional change in the statistical one-sigma error bar [22]:

$$\sigma = \frac{1}{\sqrt{T}} \left(\frac{5\pi^2}{3H_{100}^2} \right) \left[\int_{f_{\rm min}}^{f_{\rm max}} {\rm d}f \, \frac{|\gamma(f)|^2}{P_1(f)\, P_2(f)} \right]^{-1/2} , \tag{31}$$

calculated using both the long-wavelength and exact detector response functions. (Here T is the observation time, $P_{1,2}(f)$ are the power-spectra of the detector output at the two sites, and we are assuming that the stochastic background is white—i.e., has constant power in the band $f_{\rm min}$ to $f_{\rm max}$.) Since any overall direction-independent response function (e.g., $C(f)$ or $C_{\rm pole}(f)$) enters the numerator and denominator of the integrand in (31) in the same way, the results of the comparison are the same for either a simple Michelson or a Michelson interferometer with Fabry-Perot arm cavities. As shown in table 2, the corrections associated with using the long-wavelength approximation are less than 1% at frequencies (50-150 Hz) considered in previous searches, and for the H1-V1 and L1-V1 pairs around 1 kHz. But for the H1-L1 cross-correlation around 1 kHz, the correction is 4%, comparable to the current calibration uncertainties for these searches.

7. Summary

In this paper, we have re-examined the errors due to the use of the long-wavelength approximation to the detector response, and its impact on current searches for gravitational waves with km-scale interferometers such as LIGO and VIRGO. We have extended the linear-frequency approximation analysis of Baskaran and Grishchuk [6] by comparing the long-wavelength expression for the detector response (6) to the

exact formula (15) for a simple Michelson, and we have included the transfer function of Fabry-Perot cavities (23) in the interferometer arms. We have argued for the use of exact expressions for accurate analysis of the frequency-dependence of the response, as the linear approximation breaks down for certain directions on the sky. For a simple Michelson interferometer, the error in using the long-wavelength response is primarily in phase, and can be as large as 10% of the maximum long-wavelength response (see figure 2). For a Michelson-Fabry-Perot interferometer, the combination (26) of the long-wavelength Michelson response (6) and the single-pole approximation to the Fabry-Perot transfer function (25) produces rather accurate results, effectively taking into account the missing phase factor in the long-wavelength approximation for a simple Michelson. Finally, we have used the exact and long-wavelength formulae to estimate the errors that arise from using the long-wavelength approximation in current searches for periodic gravitational waves (see figure 3) and an isotropic stochastic background (see tables 1 and 2). In almost all cases, the errors are negligible, being at the sub-percent level. The only exception is the planned H1-L1 cross-correlation search for a stochastic background around 1 kHz, where the use of the long-wavelength approximation would introduce a systematic error of approximately 4%.

Although our analysis has shown that the long-wavelength approximation for a Michelson-Fabry-Perot interferometer (26) is sufficiently accurate for searches performed so far (which have typically been for frequencies below a few kHz), planned searches at higher frequencies will require one to go beyond the long-wavelength approximation for accurate analysis. For example, the presence of Fabry-Perot cavities in the interferometer arms gives us another frequency band to search for gravitational waves. For the 4-km LIGO interferometers this is approximately a 200-Hz band centered at the FSR ($f = 37.5$ kHz). Enhanced sensitivity of the detectors (only a factor of 5-8 less than at DC, as shown in figure 1) has motivated installation of 262 kHz digitizers at both LIGO sites to produce a high-frequency gravitational-wave channel for searches of gravitational-wave signals at the FSR and 2 FSR [23]. Efforts to analyze the data from this channel during the 4th and 5th LIGO science runs are underway for both stochastic searches [24] and bursts [25, 26]. There are also plans for searches for stochastic gravitational waves at even higher frequencies (around 100 MHz) [27]. The exact expressions for the detector response functions are a must for these searches.

Acknowledgments

The authors would like to acknowledge conversations with C Cutler, S Desai, L Grishchuk, D Khurana, G Mendell, R Prix, R Savage, and G Woan. This work was supported by the Max-Planck-Society and the German Aerospace Center (DLR), and NSF grant PHY-0555842 awarded to The University of Texas at Brownsville. This paper has been assigned LIGO Document Number P080036-Z.

References

[1] Barish B C and Weiss R 1999 *Phys. Today* **52** 44
[2] Bradaschia C *et al.* 1990 *Nucl. Instrum. Methods* **289** 518
[3] Misner C W, Thorne K S and Wheeler J A 1973 *Gravitation* (San Francisco: W.H. Freeman and Company)
[4] Gürsel Y, Linsay P, Spero R, Saulson P, Whitcomb S and Weiss R 1984 in *A Study of a Long Baseline Gravitational Wave Antenna System* (National Science Foundation Report)

[5] Estabrook F 1985 *Gen. Rel. Grav.* **17** 719
[6] Baskaran D and Grishchuk L P 2004 *Class. Quantum Grav.* **21** 4041
[7] Abbott B *et al.* 2007 Ligo: The laser interferometer gravitational-wave observatory LIGO Technical Report P070082-04
[8] Schutz B F and Tinto M 1987 *Mon. Not. R. Astr. Soc.* **224** 131
[9] Thorne K 1987 *300 Years of Gravitation* (University of Chicago Press, Chicago) chap Gravitational Radiation
[10] Christensen N 1990 *On Measuring the Stochastic Gravitational Radiation Background with Laser Interferometric Antennas* Ph.D. thesis Massachusetts Institute of Technology
[11] Christensen N 1992 *Phys. Rev. D* **46** 5250
[12] Sigg D 1997 Strain calibration in LIGO. LIGO Technical Report T970101
[13] Rakhmanov M 2006 Response of LIGO 4-km interferometers to gravitational waves at high frequencies and in the vicinity of the FSR (37.5 kHz). LIGO Technical Report T060237
[14] Whelan J T 2007 Higher-frequency corrections to stochastic formulae. LIGO Technical Report T070172
[15] Schilling R 1997 *Class. Quantum Grav.* **14** 1513
[16] Larson S L, Hiscock W A and Hellings R W 2000 *Phys. Rev. D* **62** 062001
[17] Cornish N J and Rubbo L J 2003 *Phys. Rev. D* **67** 022001
[18] Dupuis R J and Woan G 2005 *Phys. Rev. D* **72** 102002
[19] Flanagan É É 1993 *Phys. Rev. D* **48** 2389
[20] Cornish N and Larson S 2001 *Class. Quantum Grav.* **18** 3473–3495
[21] Abbott B *et al.* 2007 *Phys. Rev. D* **76** 022001
[22] Allen B and Romano J 1999 *Phys. Rev. D* **59** 102001
[23] Sigg D and Savage R 2003 Analysis proposal to search for gravitational waves at multiples of the LIGO arm cavity free-spectral-range frequency LIGO Technical Report T030296
[24] Forrest C, Fricke T, Giampanis S and Melissinos A 2007 Search for a diurnal variation of the power detected at the FSR frequency. LIGO Technical Report T070228
[25] Savage R *et al.* 2006 LIGO high-frequency response to length- and gw-induced optical path length variations. LIGO Technical Report G060667
[26] Parker J 2007 Development of a high-frequency burst analysis pipeline. LIGO Technical Report T070037
[27] Nishizawa A *et al.* 2008 *Phys. Rev. D* **77** 022002